

Accepted Manuscript

Ldlr^{-/-} and *ApoE*^{-/-} mice better mimic the human metabolite signature of increased carotid intima media thickness compared to other animal models of cardiovascular disease

Jean Sébastien Saulnier-Blache, Rory Wilson, Kristaps Klavins, Delyth Graham, Ioana Alesutan, Gabi Kastenmüller, Rui Wang-Sattler, Jerzy Adamski, Michael Roden, Wolfgang Rathmann, Jochen Seissler, Christine Meisinger, Wolfgang Koenig, Joachim Thiery, Karsten Suhre, Annette Peters, Makuto Kuro-O, Florian Lang, Guido Dallmann, Christian Delles, Jakob Voelkl, Melanie Waldenberger, Jean-Loup Bascands, Julie Klein, Joost P. Schanstra

PII: S0021-9150(18)31221-8

DOI: [10.1016/j.atherosclerosis.2018.07.024](https://doi.org/10.1016/j.atherosclerosis.2018.07.024)

Reference: ATH 15631

To appear in: *Atherosclerosis*

Received Date: 28 March 2018

Revised Date: 21 June 2018

Accepted Date: 18 July 2018

Please cite this article as: Saulnier-Blache JeanSé, Wilson R, Klavins K, Graham D, Alesutan I, Kastenmüller G, Wang-Sattler R, Adamski J, Roden M, Rathmann W, Seissler J, Meisinger C, Koenig W, Thiery J, Suhre K, Peters A, Kuro-O M, Lang F, Dallmann G, Delles C, Voelkl J, Waldenberger M, Bascands J-L, Klein J, Schanstra JP, *Ldlr*^{-/-} and *ApoE*^{-/-} mice better mimic the human metabolite signature of increased carotid intima media thickness compared to other animal models of cardiovascular disease, *Atherosclerosis* (2018), doi: 10.1016/j.atherosclerosis.2018.07.024.

This is a PDF file of an unedited manuscript that has been accepted for publication. As a service to our customers we are providing this early version of the manuscript. The manuscript will undergo copyediting, typesetting, and review of the resulting proof before it is published in its final form. Please note that during the production process errors may be discovered which could affect the content, and all legal disclaimers that apply to the journal pertain.



***Ldlr*^{-/-} and *ApoE*^{-/-} mice better mimic the human metabolite signature of increased carotid intima media thickness compared to other animal models of cardiovascular disease.**

Jean Sébastien Saulnier-Blache^{1,2,#}, Rory Wilson^{3,4*}, Kristaps Klavins⁵, Delyth Graham⁶, Ioana Alesutan⁷, Gabi Kastenmüller^{8,9}, Rui Wang-Sattler^{3,4}, Jerzy Adamski¹⁰, Michael Roden^{11,12,9}, Wolfgang Rathmann^{13,9}, Jochen Seissler^{14,15}, Christine Meisinger^{4,16}, Wolfgang Koenig^{17,18}, Joachim Thiery¹⁹, Karsten Suhre²⁰, Annette Peters^{3,4,18,21}, Makoto Kuro-O²², Florian Lang²³, Guido Dallmann²⁴, Christian Delles⁶, Jakob Voelkl⁷, Melanie Waldenberger^{3,4,18,*}, Jean-Loup Bascands²⁵, Julie Klein^{1,2}, Joost P. Schanstra^{1,2}.

¹ Institute of Cardiovascular and Metabolic Disease, Institut National de la Santé et de la Recherche Médicale (INSERM), Toulouse, France.

² Université Toulouse III Paul-Sabatier, Toulouse, France.

³ Research Unit of Molecular Epidemiology, Helmholtz Zentrum München, German Research Center for Environmental Health, D-85764, Neuherberg, Germany.

⁴ Institute of Epidemiology, Helmholtz Zentrum München, German Research Center for Environmental Health, D-85764, Neuherberg, Germany.

⁵ CeMM Research Center for Molecular Medicine of the Austrian Academy of Sciences, Vienna, Austria.

⁶ Institute of Cardiovascular and Medical Sciences, University of Glasgow, Glasgow, UK.

⁷ Medizinische Klinik mit Schwerpunkt Kardiologie, Campus Virchow-Klinikum, Charité-Universitätsmedizin Berlin, Berlin, Germany.

⁸ Institute of Bioinformatics and Systems Biology, Helmholtz Zentrum München - German Research Center for Environmental Health, 85764, Neuherberg, Germany.

⁹ German Center for Diabetes Research (DZD), 85764, Neuherberg, Germany.

¹⁰ Institute of Experimental Genetics, Genome Analysis Center, Helmholtz Zentrum München, German Research Center for Environmental Health, D-85764, Neuherberg, Germany.

¹¹ Institute for Clinical Diabetology, German Diabetes Center at Heinrich Heine University, Leibniz Center for Diabetes Research, Düsseldorf, Germany.

¹² Department of Endocrinology and Diabetology, Medical Faculty, Heinrich Heine University, Düsseldorf, Germany.

¹³ German Diabetes Center, Leibniz Institute at Heinrich Heine University Düsseldorf, Institute of Biometrics and Epidemiology, Düsseldorf, Germany.

¹⁴ Diabetes Zentrum, Medizinische Klinik und Poliklinik IV – Campus Innenstadt, Klinikum der Ludwig-Maximilians-Universität München, Munich, Germany.

¹⁵ Clinical Cooperation Group Diabetes, Ludwig-Maximilians-Universität München and Helmholtz Zentrum München, Munich, Germany.

¹⁶ Chair of Epidemiology, Ludwig-Maximilians-Universität München, UNIKA-T, Augsburg, Germany.

¹⁷ Deutsches Herzzentrum München, Technische Universität München, Munich, Germany.

¹⁸ German Center for Cardiovascular Research (DZHK), Partner Site Munich Heart Alliance, Munich, Germany.

¹⁹ Institute of Laboratory Medicine, Clinical Chemistry and Molecular Diagnostics, University Hospital, Leipzig, Germany.

²⁰ Department of Physiology and Biophysics, Weill Cornell Medicine-Qatar, Education City,
PO Box 24144, Doha, Qatar.

²¹ Institute for Medical Informatics, Biometrics and Epidemiology, Ludwig-Maximilians-
Universität (LMU) Munich, Munich, Germany.

²² Center for Molecular Medicine, Jichi Medical University, Shimotsuke, Japan.

²³ Physiologisches Institut, University of Tübingen, 72076 Tübingen, Germany. Department of
Molecular Medicine II, Heinrich Heine University Duesseldorf, Duesseldorf, Germany.

²⁴ Biocrates Life Sciences AG, Eduard-Bodem-Gasse 8, 6020 Innsbruck, Austria.

²⁵ Institut National de la Sante et de la Recherche Médicale (INSERM), U1188 - Université de
La Réunion, France

Corresponding author: jean-sebastien.saulnier-blache@inserm.fr

* These authors contributed equally to this work.

Abstract

Background and aims: Preclinical experiments on animal models are essential to understand the mechanisms of cardiovascular disease (CVD). Metabolomics allows access to the metabolic perturbations associated with CVD in heart and vessels. Here we assessed which potential animal CVD model most closely mimics the serum metabolite signature of increased carotid intima-media thickness (cIMT) in humans, a clinical parameter widely accepted as a surrogate of CVD.

Methods: A targeted mass spectrometry assay was used to quantify and compare a series of blood metabolites between 1362 individuals (KORA F4 cohort) and 5 animal CVD models: *ApoE*^{-/-}, *Ldlr*^{-/-}, and klotho-hypomorphic mice (*kl/kl*) and SHRSP rats with or without salt feeding. The metabolite signatures were obtained using linear regressions adjusted for various co-variates.

Results: In human, increased cIMT [quartile Q4 vs. Q1] was associated with 26 metabolites (9 acylcarnitines, 2 lysophosphatidylcholines, 9 phosphatidylcholines and 6 sphingomyelins). Acylcarnitines correlated preferentially with serum glucose and creatinine. Phospholipids correlated preferentially with cholesterol (total and LDL). The human signature correlated positively and significantly with *Ldlr*^{-/-} and *ApoE*^{-/-} mice, while correlation with *kl/kl* mice and SHRP rats was either negative and non-significant. Human and *Ldlr*^{-/-} mice shared 11 significant metabolites displaying the same direction of regulation: 5 phosphatidylcholines, 1 lysophosphatidylcholines, 5 sphingomyelins; *ApoE*^{-/-} mice shared 10.

Conclusions: The human cIMT signature was partially mimicked by *Ldlr*^{-/-} and *ApoE*^{-/-} mice. These animal models might help better understand the biochemical and molecular

mechanisms involved in the vessel metabolic perturbations associated with, and contributing to metabolic disorders in CVD.

ACCEPTED MANUSCRIPT

Introduction

Cardiovascular disease (CVD) is the leading cause of death worldwide (1). The major clinical cardiovascular events, myocardial infarction and stroke, are the symptomatic end-stage of a number of distinct pathophysiological processes affecting both the small and large vessels. Early markers are required to develop targeted strategies to prevent pathological complications of CVD. Complex structural and functional changes leading to endothelial dysfunction, medial vascular calcification, atherosclerosis and thrombosis are induced in response to different risk factors, including smoking, dyslipidaemia, diabetes, hypertension and chronic kidney disease (2-4). Assessment of carotid intima media thickness (cIMT) is accepted as a marker of early atherosclerosis and a good predictor of cardiovascular outcomes (5, 6).

Preclinical experiments on animal models are essential to understand the mechanisms of CVD progression and to develop preventive and therapeutic treatment strategies. However, the translational value of an animal model strongly depends on its ability to robustly reproduce important functional, structural, and molecular pathological features of human disease. Various animal models have been developed as means to display different well-known risk factors for accelerated human CVD (3). Among the most frequently used are the *Ldlr*^{-/-} and *ApoE*^{-/-} mice atherosclerotic models fed with high cholesterol diet to mimic human dyslipidaemia (7-9). Similar to patients with advanced chronic kidney disease, *klotho* hypomorphic mice (*kl/kl*) develop hyperphosphatemia and extensive medial vascular calcifications (10, 11). The stroke-prone spontaneously hypertensive rat (SHRSP), obtained by selective inbreeding of the Wistar–Kyoto (WKY) strain, is a well-characterized CVD model of high blood pressure, a characteristic which can be further increased by salt feeding (7, 9).

All these animal models exhibit artery thickening due to plaque formation (*ApoE*^{-/-} and *Ldlr*^{-/-} mice), medial vascular calcification (*kl/kl* mice) or hypertension (SHRSP and SHRSP-NaCl rats). Which of these animal models best mimics increased human cIMT remains an open question.

Typically, the suitability of animal models to mimic human disease is based on phenotypic similarity (e.g. dyslipidaemia, plaque size and number, blood pressure, etc.) and, at best, a few molecular features (eg increased circulating cytokines (12) or cell adhesion molecules (13)). However, this restricted number of observations only partially describes multifactorial diseases such as CVD.

Numerous metabolic cardiac and vessel perturbations are associated with and contribute to CVD. Metabolomics gives access to the metabolite and lipid compositions of biological fluids or biopsies reflecting the metabolic signature of individual patients and may serve as a valuable diagnostic and prognostic tool to manage CVD (14-16). Metabolomics also represents an opportunity to better understand the biological processes related to development and progression of atherosclerosis.

Here we assessed which animal model most closely mimics human CVD by using a metabolomics approach. For that we analysed the blood metabolome similarities that exist between human CVD and 5 recognized animal models of vascular lesions (*ApoE*^{-/-}, *Ldlr*^{-/-}, *kl/kl* mice and SHRSP rats with or without salt feeding).

Materials and methods.

Cohort study design. The KORA study (Cooperative health research in the Region of Augsburg) consists of independent population-based samples from the general population

living in the region of Augsburg, Southern Germany. The study has been conducted according to the principles expressed in the Declaration of Helsinki. Written informed consent has been given by each participant. The informed consents given by KORA study participants does not cover data posting in public databases. However, data are available upon request from KORA gen (<https://epi.helmholtz-muenchen.de/>). Data requests can be submitted online and are subject to approval by the KORA Board. The study was reviewed and approved by the local ethics committee (Bayerische Landesärztekammer). The S4 survey (examination 1999-2001) consisted of standardized interviews, physical examinations and blood sampling. Only individuals between the ages of 25 and 74 were selected. For the current study, participants of the KORA F4 cohort (examination 2006-2008), a seven-year follow-up study of the KORA S4 cohort, were used (17).

Carotid intima media thickness (cIMT), used here as a surrogate for CVD, and the anthropometric and biological parameters of the participants were measured as previously described (17, 18). An average of the left and right cIMT was used as the variable of interest in all human models. Valid cIMT data were obtained from 2714 individuals (cIMT group). A drug-free cIMT group of 1814 was isolated from the cIMT group after exclusion of the individuals treated with statins, fibrates, beta-blockers, ACE inhibitors, nitrates, lipid-lowering drugs or anti-hypertensives. The bottom (Q1) and the top (Q4) cIMT quartiles contained 687 and 675 individuals in cIMT group, and 611 and 273 individuals in the drug-free cIMT group. Sample characteristics of the individuals of the bottom (Q1) and the top (Q4) cIMT quartiles can be found in **Table 1**.

Lipid levels were determined in fasting fresh blood samples at most six hours after collection. In KORA F4 total cholesterol was measured using the cholesterol-esterase method (CHOL Flex, Dade-Behring, Germany). HDL and triglyceride levels were determined

using the TGL Flex and AHDL Flex methods (Dade-Behring, Germany), respectively, and LDL was measured by a direct method (ALDL, Dade-Behring, Germany). In KORA F4 the intra-assay coefficient of variation (CV) for repeated measurements was 1.85% (total cholesterol), 2.75% (triglycerides), 3.25% (HDL-C) and 2.7% (LDL-C).

Animal models of CVD. *ApoE*^{-/-} (n=23) and *Ldlr*^{-/-} (n=22) and their wild-type controls (C57Bl6J; n=20) mice were purchased from Charles River at the age of 5 weeks. *ApoE*^{-/-} and *Ldlr*^{-/-} mice were fed a high cholesterol diet (1.2% of cholesterol, 6% fat and 2% sucrose (Ssniff, Soest, Germany) diet: TD.96335 mod. – 1.25 % cholesterol) from the age of 8 weeks to sacrifice (22 weeks). C57Bl6J mice were fed a regular chow all along the protocol. Blood samples were collected and stored at -80°C. The project was approved by the local (Inserm/UPS US006 CREFRE) and national ethics committees under the number 02604.02. *ApoE*^{-/-} and *Ldlr*^{-/-} mice exhibited dyslipidaemia (increased total cholesterol, LDL-cholesterol and triglycerides) when compared to controls, as previously described (7, 9).

Kl/kl mice (n=10) and their corresponding wild-type mice (129Sv) (n=10) were described previously (19). Mice were fed a standard rodent chow and drinking water ad libitum. Mice were sacrificed at 7 weeks of age, and blood was collected and stored at -80°C. All animal experiments were conducted according to the recommendations of the Guide for Care and Use of Laboratory Animals of the National Institutes of Health as well as the German law for the welfare of animals, and reviewed and approved by the local government authority.

Inbred colonies of stroke-prone spontaneously hypertensive rats (SHRSP; n=28) and normo-tensive Wistar Kyoto rats (WKY; n=13) have been maintained at the University of Glasgow since 1991, as previously described (20, 21). Animals were housed under controlled conditions, fed standard rat chow (rat and mouse No. 1 maintenance diet, Special Diet

Services) and water ad libitum. At 18 weeks of age, SHRSP rats were administered 1% NaCl in their drinking water (SHRSP-NaCl; n=14) or provided with regular water (SHRSP; n=14) for three weeks. WKY rats (n=13) were maintained under regular water. Blood samples were collected at sacrifice (21 weeks) and stored at -80°C. All animal procedures were approved by the Home Office according to the Animals (Scientific Procedures) Act 1986, under Project Licence 7009021. SHRSP and SHRSP-NaCl rats showed increased systolic blood pressure and cardiac hypertrophy when compared to their control WKY rats as previously described (20, 21).

Metabolite quantification in human and animal. A series of metabolites was quantified (μM) in serum samples from individuals of the KORA F4 cohort and in plasma from the animal models using a targeted quantitative and quality controlled metabolomics approach based on electrospray ionization tandem mass spectrometry with the Absolute/IDQ™p150 (human) and Absolute/IDQ™p180 (animals) kits (BIOCRATES Life Sciences AG, Innsbruck, Austria). Details of measurement, quality control and imputation of the KORA samples have been previously published (22). Sample preparation was performed according to the user manual. Samples were randomized, and multiple quality control samples were included in the measurement sequence. In animals, values lower than the limit of detection (LOD) were set to half the value of the LOD for that metabolite. More details about mass spectrometry measurements and data analysis have been previously described (23, 24) (25). The p180kit corresponds to the p150kit completed with biogenic amines and biliary acids. These 2 classes of metabolites were not considered to compare human and animals. A list of the metabolites and their abbreviations is given in **Supplementary Table 1**. The number of metabolites that passed quality control was 151 for human and 167 for the animal models;

149 metabolites were common between human and animals. Abbreviations of the metabolite classes are: ACs (acylcarnitines), AAs (amino acids), PCs (phosphatidylcholines), lysoPCs (lysophosphatidylcholines), SM (sphingomyelins). A further 16 metabolite sums and ratios were previously identified to be of interest and added to the dataset.

Comparison of metabolite concentrations. Differences (% variation) in metabolite concentrations (μM) between groups were analysed using two-tailed unpaired Welch's t-tests (Prism 6, GraphPad), with statistical significance judged as a false discovery rate (FDR)-adjusted p value smaller than 5%.

Regression analysis. Regression analyses were conducted by running linear regressions using R version 3.4.0 (<https://www.R-project.org/>) to take into account possible confounding factors in humans. The level of statistical significance was 5% (FDR-adjusted p value). The following comparisons were considered: Q4 vs Q1 in human cIMT and drug-free cIMT groups; *ApoE*^{-/-} vs C57Bl6J mice; *Ldlr*^{-/-} vs C57Bl6J mice; *kl/kl* vs 129Sv mice; SHRSP vs WKY rats; SHRSP-NaCl vs WKY rats.

For cIMT and drug-free cIMT, the linear regression model (m1) was: "scale(log(metabolite concentration)) = cIMT (1st/4th quartiles, reference 1st) + age + sex + batch + BMI + smoking habit (current/ex/never) + alcohol consumption (g/day) + physical activity (active yes/no)" where batch is a variable indicating the batch in which the metabolites were analysed (2 batches total). The metabolite concentrations were natural log-transformed and scaled over all individuals. Due to missing data in the covariates, for the regression analysis 13 individuals were lost for the cIMT group (7 from Q1, 6 from Q4); and 8 from the drug-free cIMT group (6 from Q1, 2 from Q4).

For *ApoE*^{-/-} and *Ldlr*^{-/-} mice, the linear regression model was “scale(log(metabolite concentration)) = mouse model” where “mouse model” is a categorical variable indicating the model in question (*ApoE*^{-/-} or *Ldlr*^{-/-}) or the reference C57Bl6J mice. Scaling was done with reference to all knock-out mouse data together.

For rats, the linear regression model was “scale(log(metabolite concentration)) = rat model” where “rat model” is a categorical variable indicating the model in question (SHSRP or SHSRP-NaCl) or the reference WKY rats administered with regular water. Scaling was done with reference to all rat data together.

For *kl/kl* mice, the model was “scale(log(metabolite concentration)) = *kl/kl* mouse model + sex” where “*kl/kl* mouse model” is a categorical variable indicating either the hypomorphic *kl/kl* models or the reference WT model. Scaling was performed with reference to all *kl/kl* mouse data together.

The metabolite concentrations were natural log-transformed and scaled, with scaling performed over all animal models. Scaling was performed to enable better comparisons between the metabolites.

Results.

Human clinical parameters. In the cIMT and drug-free cIMT groups, increased cIMT between the top and bottom quartiles (Q4 and Q1) was accompanied by significant increase in age, body mass index, and alcohol consumption, as well as by significant higher blood parameters (glucose, pressure, cholesterol, triglyceride, creatinine) although these parameters remained within a healthy range (**Table 1**).

Human metabolite signature. Comparing serum metabolite concentrations (μM) between the top and bottom cIMT quartiles (Q4 and Q1) revealed 131 and 109 metabolites (including sums and ratios) that differed significantly (FDR-adjusted $p < 0.05$) in the cIMT and drug-free cIMT groups, respectively (**Supplementary Table 2**). The relative order of variation of the different classes of metabolites was ACs>H1>SMs>AAs>PCs>lysoPCs and ACs>SMs>H1>AAs>lysoPCs>PCs for cIMT and drug-free cIMT groups respectively (**Supplementary Table 3**).

Regression analysis of the cIMT group showed that 26 metabolites (9 ACs, 2 lysoPCs, 9 PCs and 6 SMs) associated significantly with cIMT (FDR adjusted $p < 0.05$) after adjustment of various potential confounders (model m1) (**Table 2 and Supplementary Table 4**). Pearson correlation showed that ACs preferentially correlated with plasma glucose and creatinine, while PCs and SMs preferentially correlated with total cholesterol and LDL-cholesterol (**Supplementary Fig. 1**).

When running the regression after having introduced serum LDL into model m1, 8 metabolites (3 PCs, 5 SMs) lost significance (**Supplementary Table 5**). Loss of significant metabolites (3 PCs, 2 SMs) was also observed by introducing serum total cholesterol separately into model m1 (**Supplementary Table 5**). Introducing other clinical parameters, including glycemia, did not reduce, or only marginally reduced, the number of significant metabolites (**Supplementary Table 5**). When running model m1 in the drug-free cIMT group with the initial 26 significant metabolites, 6 of them lost significance (5 PCs, 1 lysoPC, FDR correction based on only the 26 significant metabolites) (**Supplementary Table 5**). These results demonstrate that LDL, total cholesterol and medication partially drive the association of some metabolites (some PCs and most SMs) with cIMT.

Metabolite signatures of the animal models. In animals, plasma concentrations (μM) of 108, 125, 77, 68 and 29 metabolites (including sums and ratios) were significantly (FDR-adjusted $p < 0.05$) different in *ApoE*^{-/-}, *Ldlr*^{-/-}, *kl/kl*, SHRSP and SHRSP-NaCl, respectively, compared to their respective controls (**Supplementary Table 2**). The relative order of level change of the different classes of metabolites was SM>PC>AC>lysoPC>AA>H1, SM>PC>lysoPC>AC>AA>H1, AA=PC>SM>AC>lysoPC>H1, AC>lysoPC>AA>H1>PC>SM and PC>=AC>lysoPC>=AA>SM>H1 in *ApoE*^{-/-}, *Ldlr*^{-/-}, *kl/kl*, SHRSP and SHRSP-NaCl, respectively (**Supplementary Table 3**).

Comparison between human and mouse models. To determine which animal model most closely mimics the human cIMT signature, the differences in metabolite concentrations in the animal models were analysed by linear regression (**Supplementary Table 4**). The Spearman correlations were then calculated between these linear regression coefficients and those obtained in humans (cIMT group) (**Fig. 1**). When taking into account all metabolites regardless of their significance, coefficients correlated positively and significantly between human and *Ldlr*^{-/-} ($p < 0.0001$) ($r = 0.27$, $p < 0.002$); positively with *ApoE*^{-/-} mice ($r = 0.13$, $p = 0.14$); and negatively and non-significantly with *kl/kl* mice ($r = -0.12$, $p = 0.17$), and with SHRSP ($r = -0.01$, $p = 0.93$) and SHRSP-NaCl rats ($r = -0.08$, $p = 0.37$) (**Fig. 1**). When considering all metabolites with a nominal $p < 0.05$ in humans (45 metabolites), the results are similar ($r = 0.42$, $p = 0.025$; $r = 0.18$, $p = 0.34$; $r = -0.14$, $p = 0.47$; $r = -0.14$, $p = 0.48$; $r = -0.14$, $p = 0.47$); and when considering only those 26 metabolites with FDR-adjusted $p < 0.05$ in human, none achieve significance but the effect sizes remain roughly unchanged.

For the 26 significant metabolites in humans, *Ldlr*^{-/-} mice display 11 (5PCs, 1 lysoPC, 5SMs) significant metabolites showing the same regulation direction (i.e. 42% of the metabolite signature of humans) (**Table 2**) and *ApoE*^{-/-} mice 10 (38%, 5PCs, 5SMs); *KI*/*kl*, SHSRP and SHSRP-NaCl shared 5, 2 and 3 (19%, 8%, 12%) significant metabolites showing concordant direction with the cIMT group, respectively. If one discounts the statistical significance of the metabolites for the animal models (ie, one looks only at the directions of association of the 26 metabolites in the animal models), the rats and klotho mice show better concordance, but remain below the levels of the *Ldlr*^{-/-} and *ApoE*^{-/-} mice.

Discussion

In the present study, we revealed a series of blood metabolites [phospholipids (PCs, lysoPCs, SMs) and acylcarnitines (ACs)] associated with elevated human cIMT. We also found that, among several animal models of vascular lesions, *Ldlr*^{-/-} and *ApoE*^{-/-} mice are those that better mimic the human cIMT signature.

Phospholipids (glycerophospholipids and sphingophospholipids) are structural constituents of cell membranes, and major components of circulating lipoproteins. LDL particles are enriched with ceramide and SM, while HDL particles are enriched with phosphatidylcholine, phosphatidylethanolamine, and phosphatidylethanolamine-based plasmalogens (26). Changes in blood phospholipids reflect alteration of lipoprotein metabolism. PCs are glycerophospholipids with choline as a head group, and they are involved in phospholipid metabolism, cell signaling, membrane structure and cell energy and are mostly influenced by diet (27). SMs accumulate in atherosclerotic lesions and plasma in

dyslipidaemia and can be used to predict acute coronary syndrome (27-29). LysoPCs are mainly produced by lipoprotein-associated phospholipase A2 (30) and are major determinants of the pro-atherogenic activity of oxidized LDL (oxLDL) and increase proteoglycan synthesis, an important determinant of intimal thickening (31). We found that all the phospholipids present in the human cIMT signature are increased and correlated preferentially with total cholesterol and LDL cholesterol, two major risk factors for the development of atherosclerosis. In our participants, increased cIMT is accompanied by a reduction of HDL cholesterol and an increase in plasma LDL-cholesterol. Although these biological parameters remain within a healthy range, their significant change might reflect a pre-dyslipidaemia that might explain the increase in some of the blood phospholipids.

ACs are intermediates of fatty acid oxidation and their elevation in blood is indicative of impaired β -oxidation and has been associated with increased risk of obesity, insulin resistance, and type 2 diabetes, all recognized as risk factors of CVD (32, 33). We also observed that increased cIMT is accompanied by increased BMI, glycaemia, HOMA-IR and HbA1c. Although these parameters remain within the normal reference, their increase might nevertheless explain the elevation of blood ACs associated with increased cIMT.

The 5 animal models of CVD that were compared to human were all expected to exhibit artery thickening due to plaque formation (*ApoE*^{-/-} and *Ldlr*^{-/-} mice), medial vascular calcification (*kl/kl*) or hypertension (SHRSP and SHRSP-NaCl rats). Nevertheless, *Ldlr*^{-/-} and *ApoE*^{-/-} mice are those that better mimicked the human cIMT signature. This is in agreement with the fact that atherosclerosis is the leading cause of cIMT elevation and arterial stiffness, due to lipid accumulation in the intima of vessel artery leading to calcification and plaque formation (34). We observed that *Ldlr*^{-/-} correlated better than *ApoE*^{-/-} with the human

cIMT signature. This is in agreement with the literature indicating that in human and *Ldlr*^{-/-}, plasma cholesterol is mostly carried by LDL particles (35). Moreover, as in humans the development of atherosclerosis in the *Ldlr*^{-/-} mouse is mainly due to dyslipidaemia, while atherosclerosis in *ApoE*^{-/-} mice is also strongly associated with inflammation (8). Most of the metabolites that correlate between KORA study and *Ldlr*^{-/-} mice are likely integral components of LDL particles (i.e. phospholipids and sphingolipids).

In contrast to *ApoE*^{-/-} and *Ldlr*^{-/-} mice, *kl/kl* mice and SHRSP rats did not mimic the human signature. *Kl/kl* mice exhibit medial vascular calcification, which develops due to hyperphosphatemia, comparable to the mineral bone disorder of chronic kidney disease patients (36, 37). Medial vascular calcification differs from atherosclerosis, although overlapping inflammatory pathways may exist (38). SHRSP is a model of arteriosclerosis secondary to high blood pressure (20, 21). Blood pressure was significantly elevated in the human cohort (4th quartile cIMT), but remained within a normal range. That might explain why we found a poor overlap with human cIMT. The current observations suggest that the metabolite signature strongly differs between atherosclerosis and medial vascular calcification due to hyperphosphatemia or chronic hypertension.

While we retrieved almost all the phospholipids (PCs, lysoPCs and SMs) of the human cIMT signature in *Ldlr*^{-/-} and *ApoE*^{-/-} signatures, we retrieved only 1 AC. As mentioned above, changes in blood phospholipids reflect alteration of lipoproteins metabolism, while increased levels of acylcarnitines are indicative of impaired β -oxidation and relate to increased risk of obesity, insulin resistance, and type 2 diabetes. *ApoE*^{-/-} and *Ldlr*^{-/-} are characterized by extensive atherosclerosis and dyslipidaemia (high plasma cholesterol and LDL cholesterol) but display no increase in body weight or glycaemia (7, 9). That might explain why blood ACs did not change in *ApoE*^{-/-} and *Ldlr*^{-/-} mice.

The fact that the hypercholesterolemia models *Ldlr*^{-/-} and *ApoE*^{-/-} mice better mimic the human metabolite profile was expected since LDL cholesterol is a major contributor to atherosclerosis development in humans. Nevertheless, we cannot exclude that knocking out LDLR or ApoE genes might have an influence on plasma metabolites independently of hypercholesterolemia.

One possible limitation of the present work is that we compared serum in human to plasma in animals. The coagulation cascade is indeed different between serum and plasma and could influence the concentrations of metabolites in these fluids. Nevertheless, we previously demonstrated that serum indeed contains higher concentrations of metabolites than plasma, but their topologies are very similar, with a high degree of correlation between the two fluids (39, 40). Therefore, while comparisons of the absolute concentrations of the metabolites can hardly be made, comparing the relative metabolite profiles between human serum and animal plasma is justifiable. Another limitation of the present work is that we screened a defined and limited number of metabolites due to the assay kits that were used. For example, some phosphatidylethanolamine species (not included in our assay kits) are increased in plasma from patients with non-calcified plaque with a possible association with de novo lipogenesis and type 2 diabetes (41, 42, 43) and are relatively abundant in the VLDL-fraction of lipoprotein (44). Therefore, it might be interesting to validate our findings by using other targeted or non-targeted metabolomics approaches to get access to a larger set of metabolites.

In conclusion, our work provides evidence that *Ldlr*^{-/-} and *ApoE*^{-/-} mice are interesting models to help better understanding the biochemical and molecular mechanisms involved in the vessel metabolic perturbations associated with and contributing to metabolic disorders

in CVD. These preclinical models should help in developing new preventive and therapeutic treatment strategies in human.

Conflict of interest

The authors declared they do not have anything to disclose regarding conflict of interest with respect to this manuscript.

Financial support

The KORA study was initiated and financed by the Helmholtz Zentrum München – German Research Center for Environmental Health, which is funded by the German Federal Ministry of Education and Research (BMBF) and by the State of Bavaria. The work was supported by grants from: grant agreement n°603288 (SysVasc) from the European Union Seventh Framework Programme (FP7/2007-2013); the Institut National de Santé et de Recherche Médicale (INSERM), France; the BHF Centre of Research Excellence Award RE/13/5/30177.

Authors' contributions

All authors participated in the conception and design, or analysis and interpretation of the data, contributed to drafting and revising the manuscript, and gave final approval of the version to be published.

Legends of Figures

Figure 1. Spearman correlations of the linear regression coefficients calculated for humans (Q4 vs. Q1 of cIMT) and those calculated for *ApoE*^{-/-}, *Ldlr*^{-/-}, *kl/kl*, SHRSP and SHRSP-NaCl vs. their respective controls. *r* (Spearman *r*); *p* (*p* value).

References.

1. Heusch G, Libby P, Gersh B, Yellon D, Bohm M, Lopaschuk G, et al. Cardiovascular remodelling in coronary artery disease and heart failure. *Lancet*. 2014 May 31;383(9932):1933-43. PubMed PMID: 24831770. Pubmed Central PMCID: 4330973.
2. Brown RA, Shantsila E, Varma C, Lip GY. Current Understanding of Atherogenesis. *The American journal of medicine*. 2017 Mar;130(3):268-82. PubMed PMID: 27888053.
3. von Scheidt M, Zhao Y, Kurt Z, Pan C, Zeng L, Yang X, et al. Applications and Limitations of Mouse Models for Understanding Human Atherosclerosis. *Cell metabolism*. 2017 Feb 7;25(2):248-61. PubMed PMID: 27916529. Pubmed Central PMCID: 5484632.
4. Lang F, Ritz E, Alesutan I, Voelkl J. Impact of aldosterone on osteoinductive signaling and vascular calcification. *Nephron Physiology*. 2014;128(1-2):40-5. PubMed PMID: 25377380.
5. Polak JF, Pencina MJ, Pencina KM, O'Donnell CJ, Wolf PA, D'Agostino RB, Sr. Carotid-wall intima-media thickness and cardiovascular events. *The New England journal of*

medicine. 2011 Jul 21;365(3):213-21. PubMed PMID: 21774709. Pubmed Central PMCID: 3153949.

6. Centurion OA. Carotid Intima-Media Thickness as a Cardiovascular Risk Factor and Imaging Pathway of Atherosclerosis. *Critical pathways in cardiology*. 2016 Dec;15(4):152-60. PubMed PMID: 27846007.

7. Graham D, McBride MW, Gaasenbeek M, Gilday K, Beattie E, Miller WH, et al. Candidate genes that determine response to salt in the stroke-prone spontaneously hypertensive rat: congenic analysis. *Hypertension*. 2007 Dec;50(6):1134-41. PubMed PMID: 17938382.

8. Getz GS, Reardon CA. Animal models of atherosclerosis. *Arteriosclerosis, thrombosis, and vascular biology*. 2012 May;32(5):1104-15. PubMed PMID: 22383700. Pubmed Central PMCID: 3331926.

9. Koh-Tan HH, Dashti M, Wang T, Beattie W, McClure J, Young B, et al. Dissecting the genetic components of a quantitative trait locus for blood pressure and renal pathology on rat chromosome 3. *Journal of hypertension*. 2017 Feb;35(2):319-29. PubMed PMID: 27755386. Pubmed Central PMCID: 5214373.

10. Kuro-o M, Matsumura Y, Aizawa H, Kawaguchi H, Suga T, Utsugi T, et al. Mutation of the mouse *klotho* gene leads to a syndrome resembling ageing. *Nature*. 1997 Nov 6;390(6655):45-51. PubMed PMID: 9363890.

11. Kurosu H, Yamamoto M, Clark JD, Pastor JV, Nandi A, Gurnani P, et al. Suppression of aging in mice by the hormone *Klotho*. *Science*. 2005 Sep 16;309(5742):1829-33. PubMed PMID: 16123266. Pubmed Central PMCID: 2536606.

12. Kleemann R, Zadelaar S, Kooistra T. Cytokines and atherosclerosis: a comprehensive review of studies in mice. *Cardiovascular research*. 2008 Aug 1;79(3):360-76. PubMed PMID: 18487233. Pubmed Central PMCID: 2492729.
13. Soliman A, Kee P. Experimental models investigating the inflammatory basis of atherosclerosis. *Current atherosclerosis reports*. 2008 Jun;10(3):260-71. PubMed PMID: 18489855.
14. Laaksonen R. Identifying new Risk Markers and Potential Targets for Coronary Artery Disease: The Value of the Lipidome and Metabolome. *Cardiovascular drugs and therapy*. 2016 Feb;30(1):19-32. PubMed PMID: 26896184.
15. Dona AC, Coffey S, Figtree G. Translational and emerging clinical applications of metabolomics in cardiovascular disease diagnosis and treatment. *European journal of preventive cardiology*. 2016 Oct;23(15):1578-89. PubMed PMID: 27103630.
16. Ussher JR, Elmariah S, Gerszten RE, Dyck JR. The Emerging Role of Metabolomics in the Diagnosis and Prognosis of Cardiovascular Disease. *Journal of the American College of Cardiology*. 2016 Dec 27;68(25):2850-70. PubMed PMID: 28007146.
17. Kowall B, Ebert N, Then C, Thiery J, Koenig W, Meisinger C, et al. Associations between blood glucose and carotid intima-media thickness disappear after adjustment for shared risk factors: the KORA F4 study. *PloS one*. 2012;7(12):e52590. PubMed PMID: 23285104. Pubmed Central PMCID: 3528645.
18. Pfeiffer L, Wahl S, Pilling LC, Reischl E, Sandling JK, Kunze S, et al. DNA methylation of lipid-related genes affects blood lipid levels. *Circulation Cardiovascular genetics*. 2015 Apr;8(2):334-42. PubMed PMID: 25583993. Pubmed Central PMCID: 5012424.
19. Leibrock CB, Alesutan I, Voelkl J, Pakladok T, Michael D, Schleicher E, et al. NH₄Cl Treatment Prevents Tissue Calcification in Klotho Deficiency. *Journal of the American Society*

of Nephrology : JASN. 2015 Oct;26(10):2423-33. PubMed PMID: 25644113. Pubmed Central PMCID: 4587682.

20. Jeffs B, Negrin CD, Graham D, Clark JS, Anderson NH, Gauguier D, et al. Applicability of a "speed" congenic strategy to dissect blood pressure quantitative trait loci on rat chromosome 2. Hypertension. 2000 Jan;35(1 Pt 2):179-87. PubMed PMID: 10642295.

21. Koh-Tan HH, McBride MW, McClure JD, Beattie E, Young B, Dominiczak AF, et al. Interaction between chromosome 2 and 3 regulates pulse pressure in the stroke-prone spontaneously hypertensive rat. Hypertension. 2013 Jul;62(1):33-40. PubMed PMID: 23648703.

22. Ried JS, Baurecht H, Stuckler F, Krumsiek J, Gieger C, Heinrich J, et al. Integrative genetic and metabolite profiling analysis suggests altered phosphatidylcholine metabolism in asthma. Allergy. 2013;68(5):629-36. PubMed PMID: 23452035.

23. Koal T, Klavins K, Seppi D, Kemmler G, Humpel C. Sphingomyelin SM(d18:1/18:0) is significantly enhanced in cerebrospinal fluid samples dichotomized by pathological amyloid-beta₄₂, tau, and phospho-tau-181 levels. Journal of Alzheimer's disease : JAD. 2015;44(4):1193-201. PubMed PMID: 25408209. Pubmed Central PMCID: 4699259.

24. Klavins K, Koal T, Dallmann G, Marksteiner J, Kemmler G, Humpel C. The ratio of phosphatidylcholines to lysophosphatidylcholines in plasma differentiates healthy controls from patients with Alzheimer's disease and mild cognitive impairment. Alzheimer's & dementia. 2015 Sep 2;1(3):295-302. PubMed PMID: 26744734. Pubmed Central PMCID: 4700585.

25. St John-Williams L, Blach C, Toledo JB, Rotroff DM, Kim S, Klavins K, et al. Targeted metabolomics and medication classification data from participants in the ADNI1 cohort.

Scientific data. 2017 Oct 17;4:170140. PubMed PMID: 29039849. Pubmed Central PMCID: 5644370.

26. Kolovou G, Kolovou V, Mavrogeni S. Lipidomics in vascular health: current perspectives. *Vascular health and risk management*. 2015;11:333-42. PubMed PMID: 26109865. Pubmed Central PMCID: 4472029.

27. Chen Y, Wen S, Jiang M, Zhu Y, Ding L, Shi H, et al. Atherosclerotic dyslipidemia revealed by plasma lipidomics on ApoE(-/-) mice fed a high-fat diet. *Atherosclerosis*. 2017 Jul;262:78-86. PubMed PMID: 28527370.

28. De Leon H, Boue S, Szostak J, Peitsch MC, Hoeng J. Systems Biology Research into Cardiovascular Disease: Contributions of Lipidomics-based Approaches to Biomarker Discovery. *Current drug discovery technologies*. 2015;12(3):129-54. PubMed PMID: 26135855.

29. Jiang XC, Paultre F, Pearson TA, Reed RG, Francis CK, Lin M, et al. Plasma sphingomyelin level as a risk factor for coronary artery disease. *Arteriosclerosis, thrombosis, and vascular biology*. 2000 Dec;20(12):2614-8. PubMed PMID: 11116061.

30. Wilensky RL, Macphee CH. Lipoprotein-associated phospholipase A(2) and atherosclerosis. *Current opinion in lipidology*. 2009 Oct;20(5):415-20. PubMed PMID: 19667981.

31. Little PJ, Ballinger ML, Osman N. Vascular wall proteoglycan synthesis and structure as a target for the prevention of atherosclerosis. *Vascular health and risk management*. 2007;3(1):117-24. PubMed PMID: 17583182. Pubmed Central PMCID: 1994044.

32. Mihalik SJ, Goodpaster BH, Kelley DE, Chace DH, Vockley J, Toledo FG, et al. Increased levels of plasma acylcarnitines in obesity and type 2 diabetes and identification of a marker

of glucolipototoxicity. *Obesity*. 2010 Sep;18(9):1695-700. PubMed PMID: 20111019. Pubmed Central PMCID: 3984458.

33. Roberts LD, Koulman A, Griffin JL. Towards metabolic biomarkers of insulin resistance and type 2 diabetes: progress from the metabolome. *The lancet Diabetes & endocrinology*. 2014 Jan;2(1):65-75. PubMed PMID: 24622670.

34. Patel AK, Suri HS, Singh J, Kumar D, Shafique S, Nicolaides A, et al. A Review on Atherosclerotic Biology, Wall Stiffness, Physics of Elasticity, and Its Ultrasound-Based Measurement. *Current atherosclerosis reports*. 2016 Dec;18(12):83. PubMed PMID: 27830569.

35. Emini Veseli B, Perrotta P, De Meyer GRA, Roth L, Van der Donckt C, Martinet W, et al. Animal models of atherosclerosis. *European journal of pharmacology*. 2017 Dec 5;816:3-13. PubMed PMID: 28483459.

36. Voelkl J, Alesutan I, Leibrock CB, Quintanilla-Martinez L, Kuhn V, Feger M, et al. Spironolactone ameliorates PIT1-dependent vascular osteoinduction in klotho-hypomorphic mice. *The Journal of clinical investigation*. 2013 Feb;123(2):812-22. PubMed PMID: 23298834. Pubmed Central PMCID: 3561808.

37. Alesutan I, Feger M, Tuffaha R, Castor T, Musculus K, Buehling SS, et al. Augmentation of phosphate-induced osteo-/chondrogenic transformation of vascular smooth muscle cells by homoarginine. *Cardiovascular research*. 2016 Jun 1;110(3):408-18. PubMed PMID: 27001421.

38. Amann K. Media calcification and intima calcification are distinct entities in chronic kidney disease. *Clinical journal of the American Society of Nephrology : CJASN*. 2008 Nov;3(6):1599-605. PubMed PMID: 18815240.

39. Suarez-Diez M, Adam J, Adamski J, Chasapi SA, Luchinat C, Peters A, et al. Plasma and Serum Metabolite Association Networks: Comparability within and between Studies Using NMR and MS Profiling. *Journal of proteome research*. 2017 Jul 7;16(7):2547-59. PubMed PMID: 28517934. Pubmed Central PMCID: 5645760.
40. Yu Z, Kastenmuller G, He Y, Belcredi P, Moller G, Prehn C, et al. Differences between human plasma and serum metabolite profiles. *PloS one*. 2011;6(7):e21230. PubMed PMID: 21760889. Pubmed Central PMCID: 3132215.
41. Kunz F, Stummvoll W. Plasma phosphatidylethanolamine--a better indicator in the predictability of atherosclerotic complications? *Atherosclerosis*. 1971 May-Jun;13(3):413-25. PubMed PMID: 5119241.
42. Meikle PJ, Wong G, Tsorotes D, Barlow CK, Weir JM, Christopher MJ, et al. Plasma lipidomic analysis of stable and unstable coronary artery disease. *Arteriosclerosis, thrombosis, and vascular biology*. 2011 Nov;31(11):2723-32. PubMed PMID: 21903946.
43. Meikle PJ, Wong G, Barlow CK, Weir JM, Greeve MA, MacIntosh GL, et al. Plasma lipid profiling shows similar associations with prediabetes and type 2 diabetes. *PloS one*. 2013;8(9):e74341. PubMed PMID: 24086336. Pubmed Central PMCID: 3785490.
44. Dashti M, Kulik W, Hoek F, Veerman EC, Peppelenbosch MP, Rezaee F. A phospholipidomic analysis of all defined human plasma lipoproteins. *Scientific reports*. 2011;1:139. PubMed PMID: 22355656. Pubmed Central PMCID: 3216620.

Table 1. Characteristics of KORA F4 participants. cIMT (carotid intima media thickness). Q1 (first quartile cIMT). Q4 (last quartile cIMT). Categorical variables are presented as N (%), with p-value for the difference between Q1 and Q4 calculated using Fisher's exact test. Continuous variables are presented as mean (standard deviation), with p-value for the difference between Q1 and Q4 calculated using Welch's t-test.

	cIMT group			drug-free cIMT group		
	Q1	Q4	P	Q1	Q4	P
Categorical characteristics						
Sex (men)	271 (39.45%)	393 (58.22%)	5.00E-12	236 (38.63%)	158 (57.88%)	1.20E-07
Current smoking	155 (22.59%)	76 (11.31%)	3.20E-08	147 (24.1%)	48 (17.71%)	0.035
Former smoking	253 (36.88%)	313 (46.58%)	0.00034	216 (35.41%)	112 (41.33%)	0.097
Physical activity (active)	369 (53.71%)	330 (49.11%)	0.093	331 (54.17%)	144 (53.14%)	0.83
Previous myocardial infarction	5 (0.73%)	39 (5.8%)	3.90E-08	0 (0%)	2 (0.74%)	0.094
Angina Pectoris	25 (3.64%)	53 (7.9%)	0.00098	17 (2.78%)	9 (3.32%)	0.67
Previous stroke	4 (0.58%)	26 (3.87%)	2.40E-05	2 (0.33%)	0 (0%)	1
Presence of cancer	19 (2.77%)	85 (12.65%)	3.00E-12	15 (2.45%)	23 (8.49%)	0.00011
Intake of anti-hypertensive medicine	64 (9.32%)	370 (54.9%)	8.30E-78	0 (0%)	0 (0%)	1
Intake of beta-blockers	41 (5.97%)	210 (31.16%)	3.10E-35	0 (0%)	0 (0%)	1
Intake of ACE-inhibitors	23 (3.35%)	162 (24.07%)	2.10E-31	0 (0%)	0 (0%)	1
Intake of statins	21 (3.06%)	147 (21.84%)	3.30E-28	0 (0%)	0 (0%)	1
Intake of fibrates	1 (0.15%)	5 (0.74%)	0.12	0 (0%)	0 (0%)	1
Intake of nitrates	0 (0%)	12 (1.78%)	0.00021	0 (0%)	0 (0%)	1

Intake of lipid-lowering drugs	23 (3.35%)	153 (22.73%)	1.10E-28	0 (0%)	0 (0%)	1
Insulin therapy	2 (0.29%)	21 (3.12%)	2.70E-05	0 (0%)	2 (0.73%)	0.095
Intake of antidiabetic medication	10 (1.46%)	66 (9.81%)	3.50E-12	3 (0.49%)	7 (2.56%)	0.012
Continuous characteristics						
Age at examination	44.01 (8.47)	67.46 (8.48)	2e-318	42.87 (7.43)	64.09 (8.85)	1.00E-128
Body mass index (kg/m ²)	25.98 (4.59)	29.14 (4.5)	1.90E-35	25.59 (4.35)	28.14 (3.91)	5.70E-17
Alcohol consumption (g/day)	12.5 (17.55)	15.22 (19.26)	0.0067	12.63 (17.99)	16.57 (20.9)	0.0074
Fasting glucose in serum (mg/dl)	91.49 (11.41)	104.97 (23.04)	1.80E-38	90.27 (9.43)	99.47 (20.13)	5.70E-12
HOMA-IR	1.57 (4.92)	3.05 (14.36)	0.017	1.45 (5)	3.46 (20.82)	0.13
HbA1c value (%)	5.36 (0.39)	5.81 (0.73)	2.10E-41	5.32 (0.31)	5.6 (0.58)	2.40E-13
Systolic blood pressure (mm Hg)	113.97 (14.93)	129.96 (19.38)	1.20E-58	113.01 (14.46)	130.18 (18.09)	2.60E-36
Diastolic blood pressure (mm Hg)	73.24 (9.2)	75.24 (10.21)	0.00015	72.79 (9.12)	77.44 (9.41)	2.20E-11
Pulse frequency (beats)	73.35 (9.38)	70.92 (10.76)	9.20E-06	73.41 (9.17)	72.16 (9.58)	0.07
Total cholesterol (mg/dl)	203.71 (37.24)	222.51 (40.66)	1.80E-18	203.02 (37.37)	234.19 (39.96)	4.90E-25
HDL cholesterol (mg/dl)	58 (14.75)	53.55 (13.48)	7.40E-09	58.31 (14.47)	55.07 (14.12)	0.0019
LDL cholesterol (mg/dl)	125.28 (33.38)	143.47 (35.97)	2.10E-21	124.62 (33.28)	154.05 (35.33)	7.30E-28
Triglycerides (mg/dl)	107.3 (91.31)	139.71 (87.92)	3.70E-11	103.14 (91.47)	135.7 (79.48)	1.20E-07
Serum creatinine (mg/dl)	0.86 (0.17)	0.96 (0.28)	1.60E-14	0.85 (0.16)	0.88 (0.16)	0.003
CKD-EPI	103.03 (14.21)	80.18 (15.95)	2.50E-135	104.75 (12.6)	87.33 (13.76)	4.40E-55
Serum albumin (g/l)	45 (3.51)	44.03 (3.11)	9.60E-08	45.13 (3.5)	44.29 (3.08)	0.00041

IMT left of A. carotis communis	0.69 (0.05)	1.05 (0.09)	0	0.69 (0.05)	1.04 (0.08)	3.80E-203
IMT right of A. carotis communis	0.7 (0.05)	1.04 (0.09)	0	0.7 (0.05)	1.03 (0.08)	5.30E-200
IMT mid A. carotis communis	0.69 (0.04)	1.05 (0.08)	0	0.69 (0.04)	1.03 (0.07)	1.70E-216

ACCEPTED MANUSCRIPT

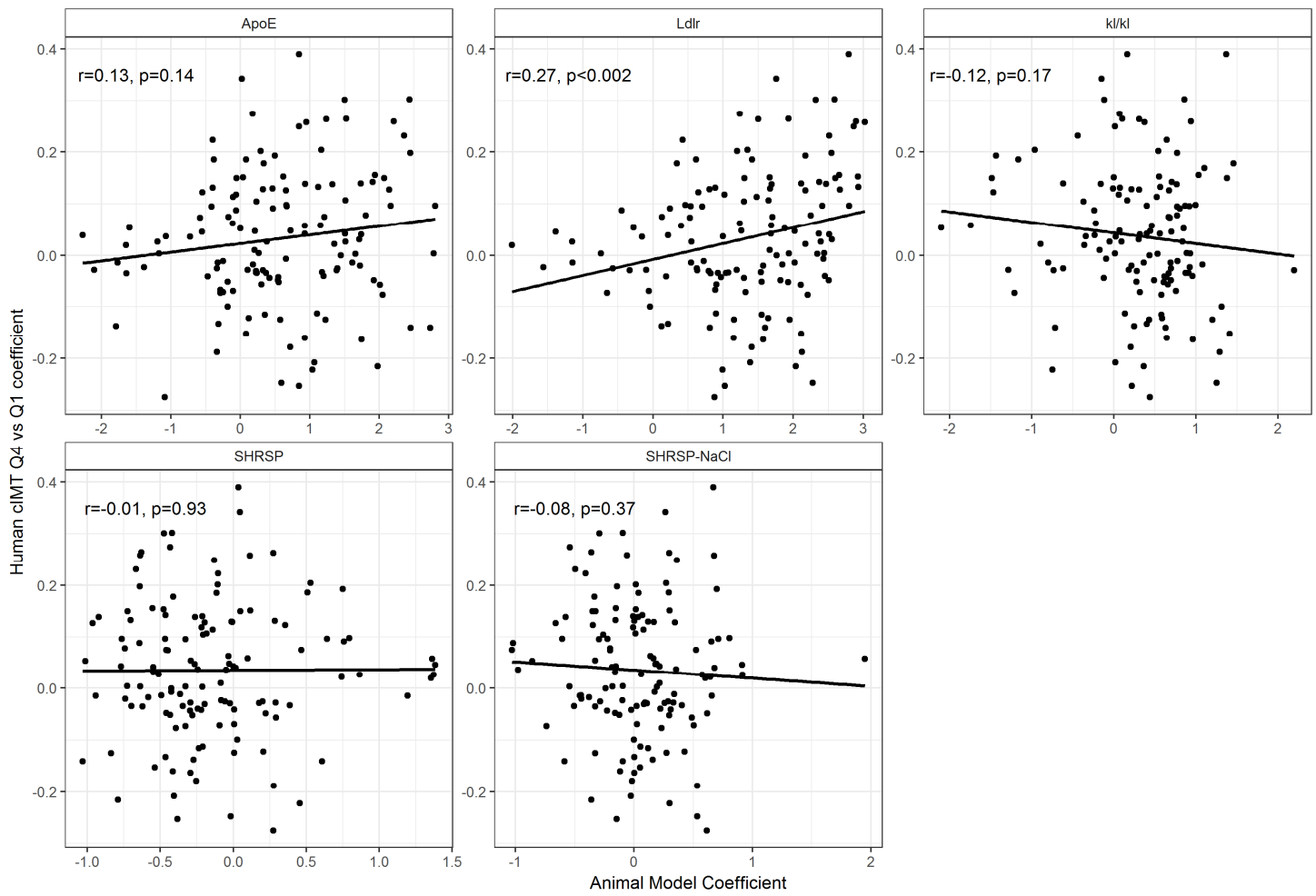


Figure 1

Highlights

- Metabolomics allows access to the metabolic perturbations associated with cardiovascular disease (CVD)
- Increased carotid intima-media thickness (cIMT) is a surrogate of CVD
- Human blood metabolite signature of increased cIMT is made of acylcarnitines and phospholipids
- *LDLR*^{-/-} and *ApoE*^{-/-} mice mimicked the phospholipid part of cIMT signature